THE JOURNAL OF PHYSICAL CHEMISTRY B

Article

pubs.acs.org/JPCB

Modeling Dynamics of Isotropic Dielectrics in a Laminar Heterogeneous Configuration

Ruel McKenzie,* Walter Zurawsky, and Jovan Mijovic

Othmer-Jacobs Department of Chemical and Biological Engineering, Polytechnic Institute of NYU, 6 MetroTech Center, Brooklyn, New York 11201, United States

ABSTRACT: The predictive capabilities of models that satisfy the Weiner bounds and Hashin−Shtrikman (HS) bounds were studied for isotropic dielectrics in a laminar heterogeneous configuration oriented perpendicular to the electric field. The dynamics were investigated isothermally using broadband dielectric relaxation spectroscopy (DRS) in the frequency range of 1 MHz to 100 mHz. The molecules chosen for study were low molecular weight glass formers, glycerol, phenyl salicylate, imidazole, and dimethyl sulfoxide, and macromolecules, polymethylhydrosiloxane, polyvinylpyrrolidone-*co*-vinyl acetate, poly-DL-lactic acid, and poly L-lactic acid. It was found that none of the models were able to adequately predict in entirety the resultant dynamics. Of the models studied, the most successful were the HS upper bound (HSUB), the complementary universal Weiner equation (CWE), and the Lichtenecker model for the dimensional parameter, $\zeta = -1/2$. The least successful models were the upper Weiner bound (UWB), the Neelakantaswamy, Turkman, and Sarkar (NTS) model for $\zeta = 1/2$, and the Lichtenecker model for $\zeta = 1/2$.

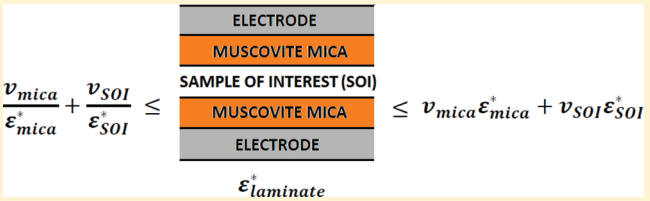

INTRODUCTION

The objective of this paper is to aid in the development and characterization of a system that serves in the analysis of dielectrics in thin films and at modified surfaces. The predictive capability of models used to describe the effect that substrates have on attaining such objectives is explored. Broadband dielectric relaxation spectroscopy (DRS) has utilized porous substrates,[1−4] atomically smooth substrates,[5−9] interdigitated electrodes,[10,11] and insulators[12−15] as probes for assessing molecular dynamics in confined geometries and at modified surfaces. When using substrates in a capacitive configuration, account should be made for the heterogeneity introduced by the substrate yet also enable the extrapolation of the dynamics for the material of interest from the heterogeneous system. To be discussed in a follow up report is the viability of a molecular interpretation for the resultant dynamics due to the presence of a substrate.

Characterization of dielectric mixtures and the study of their electromagnetic behavior has been a classical problem in dielectric theory. It was first addressed by Maxwell[16] in his treatise and later served as the most rigorous bounds for the complex apparent dielectric permittivity, ε^*_{app}, of a heterogeneous, isotropic system by Weiner:[17]

$$\left[\sum_{i=1}^{n} \frac{v_i}{\varepsilon_i^*}\right]^{-1} \leq \varepsilon^*_{app} \leq \sum_{i=1}^{n} v_i \varepsilon_i^* \tag{1}$$

Figure 1 shows that ε^*_{app} is delimited by the lower Weiner bound (LWB) on the left-hand side, where the layers are oriented perpendicular to the electric field having the components of ε^*_{app} arranged in parallel, while the right-hand side is known as the upper Weiner bound (UWB) where the layers are oriented parallel with the electric field with the components of ε^*_{app} arranged in series. The volumetric ratio of the ith component, ν_i, is equal to $d_i/\sum_i^n d_i$, where d_i is the thickness of each component. Over the century since the inception of Maxwell's heterogeneous model and Weiner's

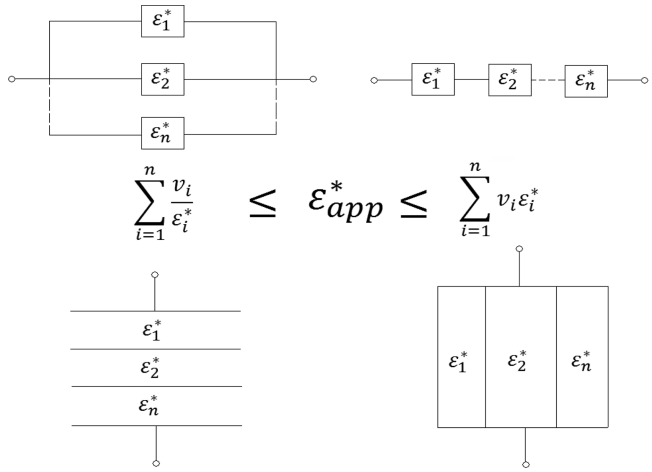

Figure 1. Maxwell's postulate and Weiner's bounds for isotropic dielectrics in a laminar heterogeneous configuration. The upper pane illustrates the electric connectivity, and the lower pane illustrates the material orientation relative to the applied electric field.

Received: November 16, 2011
Revised: March 20, 2012
Published: March 20, 2012

bounds on a heterogeneous system, numerous models have been devised to satisfy these bounds.

By the incorporation of a variational/dimensional parameter, ζ, the upper and lower Weiner bounds can be combined into a single form which shall be referred to as the universal Weiner equation (UWE) defined below as

$$\frac{\varepsilon^*_{app} - \varepsilon^*_1}{\varepsilon^*_{app} + \zeta\varepsilon^*_1} = \nu_2 \frac{\varepsilon^*_2 - \varepsilon^*_1}{\varepsilon^*_2 + \zeta\varepsilon^*_1} \tag{2}$$

This equation appears in various forms such as the Maxwell–Garnett,[18] Clausius–Mosotti,[19] and Lorenz–Lorentz[19] equations, for example. The UWE has a counterpart which shall be referred to as the complementary universal Weiner equation (CWE):

$$\frac{\varepsilon^*_{app} - \varepsilon^*_2}{\varepsilon^*_{app} + \zeta\varepsilon^*_2} = \nu_1 \frac{\varepsilon^*_1 - \varepsilon^*_2}{\varepsilon^*_1 + \zeta\varepsilon^*_2} \tag{3}$$

The UWE and CWE are defined for a two-component system. Similar to the universal Weiner equation, Bruggeman[20] suggested an effective medium approximation:

$$\sum_{i=1}^{n} \nu_i \frac{\varepsilon^*_i - \varepsilon^*_{app}}{\varepsilon^*_i + \zeta\varepsilon^*_{app}} = 0 \tag{4}$$

For the estimation of ε^*_{app}, this results in a polynomial of order n depending on the number of components in the heterogeneous system. The universal Weiner models and the Bruggeman model result in the lower Weiner bound when $\zeta = 0$ and the upper Weiner bound when $\zeta = \infty$.

Another way to satisfy the upper and lower Weiner bound was also suggested by Bruggeman[20] as a power law relation but was later generalized by Neelakantaswamy, Turkman, and Sarkar (NTS)[21] to

$$\varepsilon^*_{app} = \left(\sum_{i=1}^{n} \nu_i \varepsilon^{*\zeta}_i\right) \left(\sum_{i=1}^{n} \frac{\nu_i}{\varepsilon^*_i}\right)^{\zeta - 1} \tag{5}$$

where $0 \le \zeta \le 1$. Lichtenecker[22,23] also satisfied the bounds by the following power law relationship:

$$\varepsilon^{*\zeta}_{app} = \sum_{i=1}^{n} \nu_i \varepsilon^{*\zeta}_i \tag{6}$$

where $-1 \le \zeta \le 1$.

Hashin and Shtrikman (HS)[24,25] derived much tighter bounds on the range of values for a heterogeneous system by taking advantage of the variational approach that was initially used by Maxwell–Garnett.[18] For a binary, heterogeneous, isotropic system, the HS bounds are defined as

$$\varepsilon^*_1 + \frac{\nu_2 \varepsilon^*_1}{\frac{\varepsilon^*_1}{(\varepsilon^*_2 - \varepsilon^*_1)} + \frac{\nu_1}{\zeta}} \le \varepsilon^*_{app} \le \varepsilon^*_2 + \frac{\nu_1 \varepsilon^*_2}{\frac{\varepsilon^*_2}{(\varepsilon^*_1 - \varepsilon^*_2)} + \frac{\nu_2}{\zeta}} \tag{7}$$

In fact, the upper HS bound (UHSB) is very similar to UWE, while the lower HS bound (LHSB) is very similar to CWE. To satisfy the HS bounds, a power law relation is suggested in a form similar to the NTS model which shall be referred to as the universal HS equation (UHSE) defined below as

$$\varepsilon^*_{app} = \left[\varepsilon^*_1 + \frac{\nu_2 \varepsilon^*_1}{\frac{\varepsilon^*_1}{(\varepsilon^*_2 - \varepsilon^*_1)} + \frac{\nu_1}{\zeta_1}}\right]^{\zeta_2} \left[\varepsilon^*_2 + \frac{\nu_1 \varepsilon^*_2}{\frac{\varepsilon^*_2}{(\varepsilon^*_1 - \varepsilon^*_2)} + \frac{\nu_2}{\zeta}}\right]^{1-\zeta_2} \tag{8}$$

where $0 \le \zeta_1 \le \infty$ and $0 \le \zeta_2 \le 1$.

Investigating the dynamics of dielectric processes on ultrathin films can be accomplished by the use of substrates such as muscovite mica,[7] metalized glass slides,[6,9] and silicon wafers.[8] These are widely employed due to their smooth surface for the formation of defect free films and their capability to be used in a wide range of analytical systems. Insulators such as Teflon[12,13] and Mylar[14,15] have grown in use, albeit cautiously, due to their constant dielectric permittivity over a very wide temperature range with negligible losses. Insulators are generally used to overcome the effects of conductivity in a dielectric system, but their use for such purposes has been challenged.[26] For the purpose of this study, and going forward to the main objective, muscovite mica presents itself as a prime candidate.

This study will examine laminar dielectrics oriented perpendicular to the applied electric field. For each component, data for the models shall be generated by using experimental results for the dielectric spectra of a material of interest between aluminum electrodes while assuming that the dielectric loss of muscovite mica is negligible[7] (perfect insulator). The model results will then be compared to laminar systems of the same material of interest between muscovite mica. A wide range of chemicals from low molecular weight associating and non-associating glass formers to high molecular weight amorphous, crystallizable, and curable macromolecules is chosen to assess the predictive capabilities of the models described.

MATERIALS AND METHODS

Muscovite mica of grade V-4, 12 mm diameter, and 0.15 mm thickness was purchased from Structure Probe Incorporated (West Chester, PA). Glycerol was purchased from Life Technologies, Gibco BRL Division (Grand Island, NY). Phenyl salicylate (salol) and poly-L-lactic acid (PLLA) of MW = 700 kD were purchased from MP Biomedicals (Solon, OH). Poly-DL-lactic acid (PDLLA) of MW ~20–30 kD and polydispersity 1.8 was purchased from Polysciences, Inc. (Warrington, PA). Dimethyl sulfoxide (DMSO), imidazole, poly-1-vinyl pyrrolidone covinyl acetate (PVP-*co*-VAc) of MW = 50 kD and polymethylhydrosiloxane (PMHS) were purchased from Sigma-Aldrich (St. Louis, MO). Silica spacers of 50 μm thickness were purchased from Novocontrol GmBH and co. KG (Hundsangen, Germany).

All samples were run on a broadband dielectric spectrometer alpha analyzer (Novocontrol GmbH and Co. KG) with a Novocool temperature control module (Novocontrol GmbH and Co. KG) holding the temperature to within ±0.5 °C. The frequency range investigated was from 1 MHz to 10 mHz with the thickness of the samples between muscovite mica being 50

dx.doi.org/10.1021/jp211047j | J. Phys. Chem. B 2012, 116, 4346–4353

μm. The mesoscopic models used bulk data derived from analyzing the samples without muscovite mica at 50 μm thickness between aluminum electrodes of 12 mm diameter. Aluminum electrodes of 12 mm diameter were also used for the laminated systems. The electrodes were polished using abrasive sheets of decreasing roughness. The surface roughness of the electrodes was not obtained. Good contact between the muscovite mica and the electrodes in the sample holder was ensured. Since muscovite mica was optically transparent, checking for and removal of air bubbles was straightforward.

RESULTS AND DISCUSSION

The dynamics of the heterogeneous systems were studied over a vast temperature range as a function of frequency between 100 mHz and 1 MHz. Of particular interest to this study was the Maxwell−Wagner−Sillars (MWS) interfacial polarization[16,27,28] which is often described as being due to the difference in dielectric properties and a buildup of charge at the interface of the respective components.[29,30] The MWS interfacial polarization was perceived as polarization phenomena that occurred due to the presence of muscovite mica upon comparison to the homogeneous systems. The spectral behavior for the relaxation of MWS interfacial polarization is similar to a dipolar relaxation.[31] MWS interfacial polarization may result in the form of a relaxation process even if neither components exhibit a dipolar relaxation. From Maxwell's postulate, a system laminated perpendicular to the applied electric field should ideally result in the LWB. This presumption has often seen a direct use of the LWB without an investigation as to whether or not the system actually is represented by that model[5,7,26,32] especially if the conductivities of the components are not equal. Maxwell himself noted that some systems may not behave as his model predicts.[16] Models of such systems are usually utilized for the extraction of the dynamics of a component in the heterogeneous system, and as a result, the actual dynamics may be exaggerated. The dielectric permittivity of muscovite mica, ε_2', used was 7.1,[33] and its volumetric ratio in the heterogeneous systems was 0.857.

Figures 2a−9a compare the dynamics of the condensers with and without muscovite mica for the imaginary dielectric permittivity, ε'', and the real conductivity, σ', as a function of frequency at a temperature where a polarization phenomenon due to the presence of muscovite mica was evident. Figures 2b−9b display the model results of imaginary apparent dielectric permittivity, ε''_{app}, in the frequency domain and at a temperature where a polarization phenomenon due to the presence of muscovite mica was evident. Note however that all the molecules studied in the heterogeneous system also displayed the same molecular relaxation processes that the homogeneous system displayed but with alterations to the shape of the relaxation processes and slight shifts of the frequency of maximum loss at the same respective temperatures. Evidence of this claim is presented in Figure 5.

Glycerol when studied in a homogeneous system displayed a single relaxation process[30,34] with a concurrent single step in σ' (Figure 2a). In a laminated heterogeneous system oriented perpendicular to the applied electric field, two relaxation processes[12] are displayed. When laminated by muscovite mica, glycerol (Figure 2a) also had two relaxation processes but was different from previously published results,[12] while the observed single step in σ' from the homogeneous system is transformed to two discrete steps that encompass the same frequency range as that of the single step. Of the models

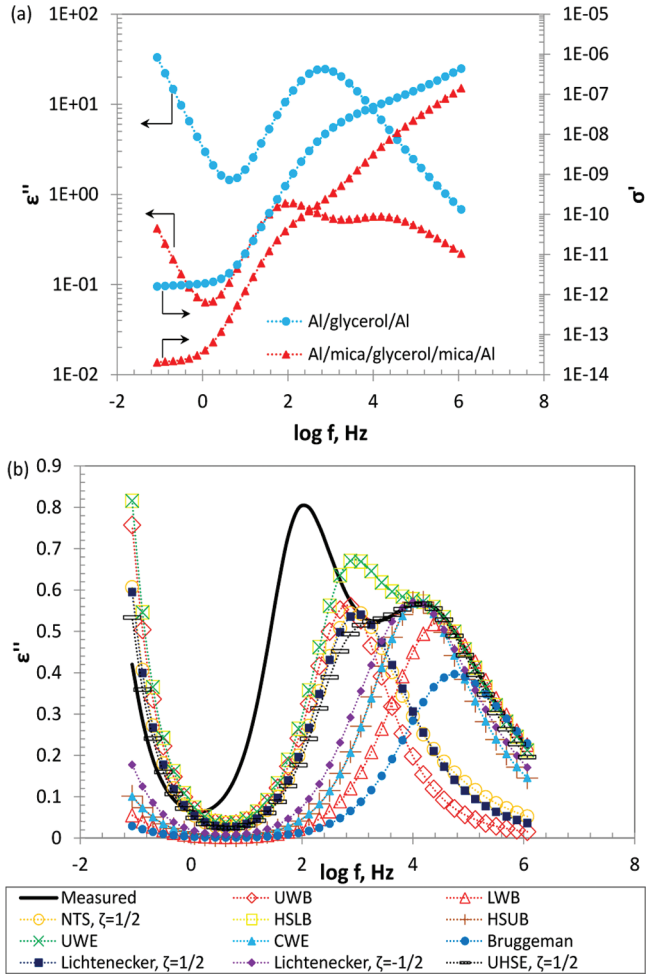

Figure 2. Dynamics of glycerol at −60 °C. (a) Imaginary dielectric permittivity, ε'', and real conductivity, σ', spectra without and with muscovite mica. (b) Comparison of model predictions for the apparent imaginary dielectric permittivity, ε''_{app}, with experimental results.

investigated (Figure 2b), the HSLB, UWE, and UHSE equations were able to correctly predict the occurrence of two relaxation processes, but they, like the rest of the models, were limited in resolving the dynamics. The faster relaxation process was resolved by the HSLB and UWE equations from the high frequency wing up to the frequency of maximum loss and the UHSE resolved the spectra of the faster relaxation process in entirety. The other models predicted a single relaxation process; the HSUB, CWE, and Lichtenecker model at $\zeta = -1/2$ were able to predict the frequency of maximum loss for the faster relaxation process but were unable to resolve the spectral shape of that process. It was not determined which process was the alpha, α, process, since the conductivity spectra showed that the homogeneous relaxation process got transformed into two processes by the presence of muscovite mica. There has been stipulation however that the slower relaxation process is due to hydrogen bonding, while the faster relaxation process is the α process.[12,13]

When imidazole was studied in a homogeneous environment in the temperature range of 100 to −80 °C, no relaxation processes were evident, only a conductivity wing (Figure 3a). To the knowledge of the authors, there has yet to be any dynamic studies of imidazole using DRS quite possibly due to

dx.doi.org/10.1021/jp211047j | J. Phys. Chem. B 2012, 116, 4346−4353

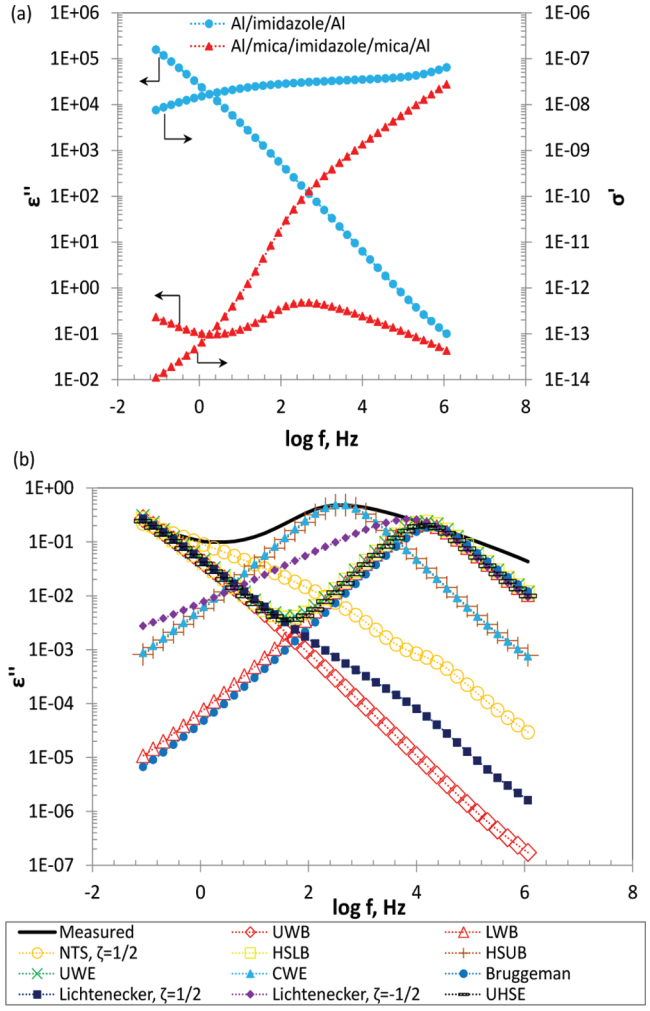

Figure 3. Dynamics of imidazole at 10 °C. (a) Imaginary dielectric permittivity, ε'', and real conductivity, σ', spectra without and with muscovite mica. (b) Comparison of model predictions for the apparent imaginary dielectric permittivity, ε''_{app}, with experimental results.

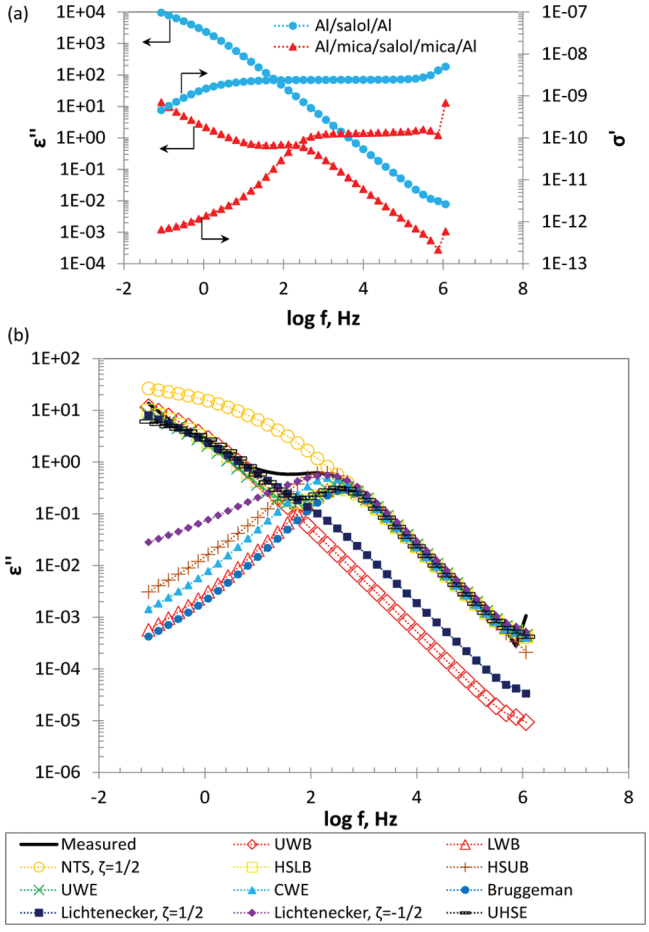

Figure 4. Dynamics of phenyl salicylate at 50 °C. (a) Imaginary dielectric permittivity, ε'', and real conductivity, σ', spectra without and with muscovite mica. (b) Comparison of model predictions for the apparent imaginary dielectric permittivity, ε''_{app}, with experimental results.

there being no presentation of a relaxation process, especially in the temperature range studied. When laminated by muscovite mica, imidazole displayed a single relaxation process that resulted in a steep step change in σ' (Figure 3a). The relaxation process could not be resolved by the models investigated (Figure 3b). The HSUB and CWE equations were able to locate the frequency of maximum loss but were unable to resolve the shape of the spectra.

The dynamics of phenyl salicylate in a homogeneous environment have been reported.[35] The published results were in the temperature range of approximately 20 to −50 °C in the frequency domain of 1 mHz to 1 GHz. Phenyl salicylate displayed a single relaxation process in the temperature range and frequency domain reported. This study scanned the temperature range from 100 to −10 °C. In this temperature range, phenyl salicylate displayed a conductivity wing in a homogeneous environment (Figure 4a), but in the laminated system (Figure 4a) a single relaxation process due to the presence of muscovite mica was observed. Most of the models, with the exception of the UWB and Lichtenecker model for ζ = 1/2, were able to resolve the high frequency wing of the relaxation process, but only the HSUB, CWE, and Lichtenecker model for ζ = −1/2 were able to locate the frequency of maximum loss for the relaxation process (Figure 4b).

DMSO has been studied in the GHz frequency domain at 25 °C and displayed a single relaxation process.[36] To observe this relaxation process in the frequency domain studied, the temperature was reduced to −100 °C. In the homogeneous system presented at −95 °C, a singular relaxation process is evident that is displayed as a step change in σ' (Figure 5a). The heterogeneous system presented a relaxation process and a polarization process, quite possibly due to the ionic characteristics of muscovite mica.[37−39] This polarization phenomenon is presented as a shoulder in the ε'' plot and a constant slope on a log scale of σ' (Figure 5a). The polarization phenomenon due to the presence of muscovite mica was slower than the relaxation process. Most of the models were able to correctly predict the location of the dielectric loss maximum but were not able to resolve the shape of the spectra (Figure 5b). None of the models were able to resolve the shoulder that occurs due to the presence of muscovite mica. If a respective model was able to correctly predict the presence of a second, slower polarization phenomenon, its location was considerably underestimated. This occurred in all the models except the UWB, NTS model for ζ = 1/2 and the Lichtenecker model for ζ = 1/2 which were only capable of predicting the occurrence of a single relaxation process.

dx.doi.org/10.1021/jp211047j | J. Phys. Chem. B 2012, 116, 4346−4353

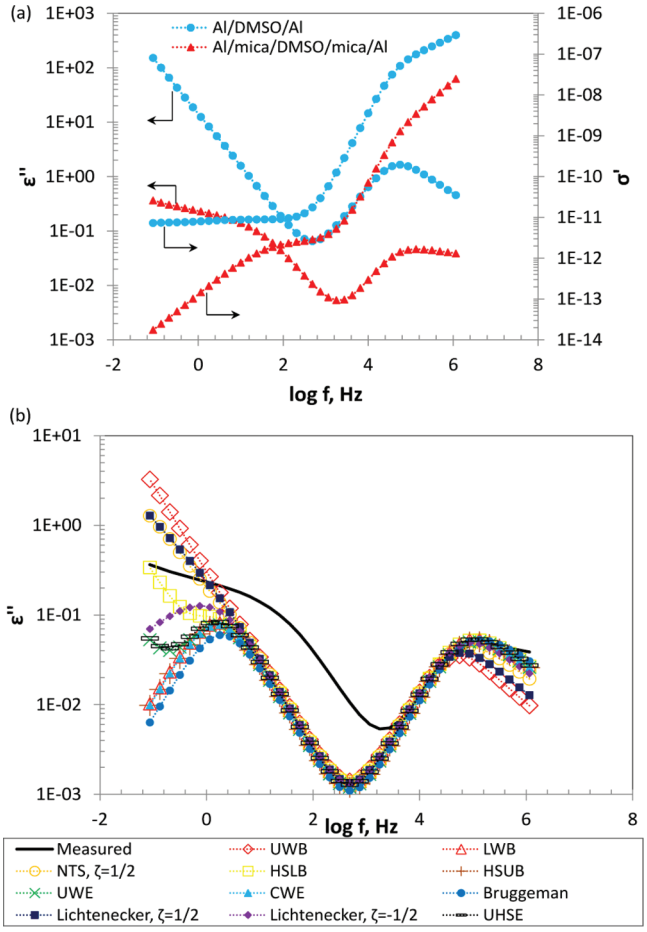

Figure 5. Dynamics of DMSO at −95 °C. (a) Imaginary dielectric permittivity, ε'', and real conductivity, σ', spectra without and with muscovite mica. (b) Comparison of model predictions for the apparent imaginary dielectric permittivity, ε''_{app}, with experimental results.

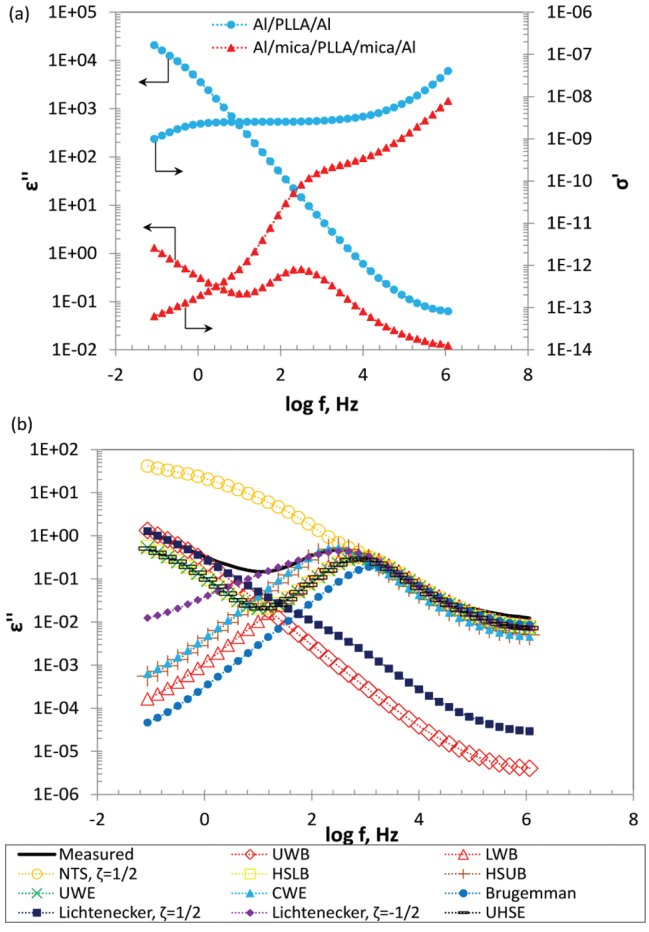

Figure 6. Dynamics of PLLA at 180 °C. (a) Imaginary dielectric permittivity, ε'', and real conductivity, σ', spectra without and with muscovite mica. (b) Comparison of model predictions for the apparent imaginary dielectric permittivity, ε''_{app}, with experimental results.

The dynamics of PLLA have been well studied.[40−42] In the frequency domain studied, PLLA does not display a relaxation process at the temperature presented for a homogeneous system but shows only a conductivity wing, while in the heterogeneous system a relaxation process is clearly evident (Figure 6a). Figure 6b presents the model results when PLLA is laminated by muscovite mica. PLLA presented a single relaxation process that was best resolved by the Lichtenecker model for $\zeta = -1/2$. The model was able to resolve the spectral shape of the relaxation process and locate the frequency of maximum loss. If a conductivity term were included in the models investigated, then the Lichtenecker model for $\zeta = -1/2$ would have been able to completely resolve the entire spectra including the low frequency conductivity wing. The frequency of maximum loss was also located by the HSUB and CWE equations, but the spectral shapes were not resolved.

Figure 7a shows that PMHS in an uncured state results in only a conductivity wing in a representation of ε'' and a plateau in σ' for a homogeneous system from 50 to −90 °C. No relaxation process was evident. For the heterogeneous system studied, no relaxation process was evident in that same temperature range either. However, similar to the polarization phenomenon that occurred with DMSO which was presented as a shoulder in the ε'' representation of the spectra (Figure 5b), σ' also goes through a transition and leads to a constant slope in log σ' which also may be due to the ionic character of muscovite mica.[37−39] The UWB, Bruggeman, and Lichtenecker model for $\zeta = 1/2$ were able to predict that no relaxation processes would occur in the heterogeneous system, while the other models predicted a single relaxation process. However, none of the models were able to resolve the dynamics of PMHS in the heterogeneous environment (Figure 7b).

From Figure 8a, PDLLA in the homogeneous system presents a conductivity wing in the ε'' spectra which presented itself as a plateau that transitions to a constant slope in the log σ' representation at the temperature presented. In the heterogeneous system, a single relaxation process due to the presence of muscovite mica is displayed that is represented by a step change in σ'. Figure 8b shows that most of the models correctly predicted a single relaxation process at the temperature presented, but only the HSUB and CWE equations were able to locate the frequency of maximum loss for the relaxation process. The other models were able to resolve the high frequency wing of the relaxation process to an extent, but the location of the frequency at which the loss was a maximum was often overestimated.

The copolymer, PVP-*co*-VAc, presented an interesting example for the dynamics in a laminated heterogeneous system because the surface properties of a substrate can influence which section of the copolymer would prefer the interface, thus

dx.doi.org/10.1021/jp211047j | J. Phys. Chem. B 2012, 116, 4346−4353

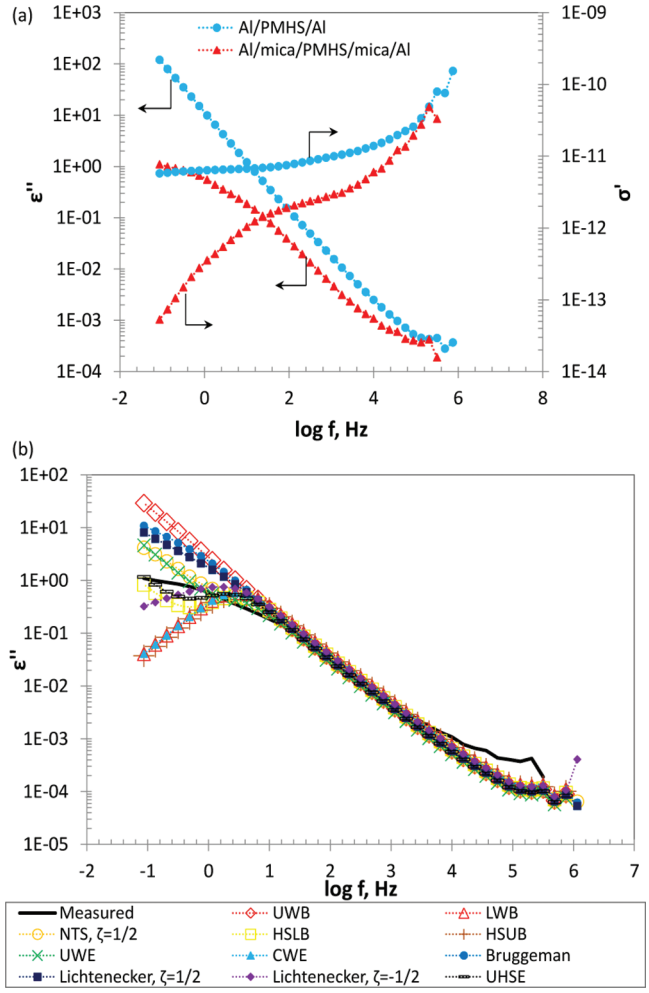

Figure 7. Dynamics of PMHS at 50 °C. (a) Imaginary dielectric permittivity, ε'', and real conductivity, σ', spectra without and with muscovite mica. (b) Comparison of model predictions for the apparent imaginary dielectric permittivity, ε''_{app}, with experimental results.

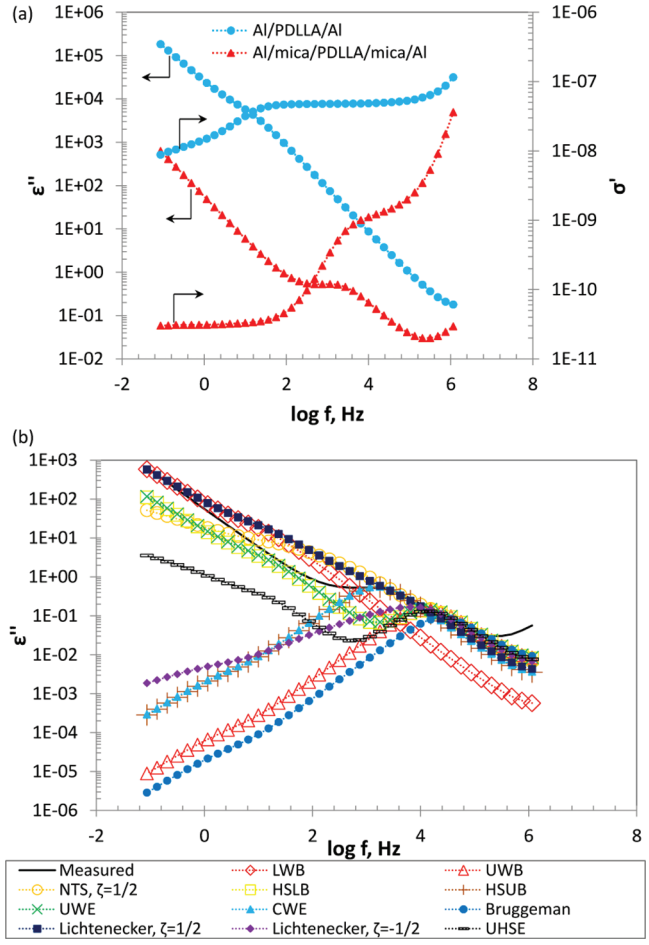

Figure 8. Dynamics of PDLLA at 130 °C. (a) Imaginary dielectric permittivity, ε'', and real conductivity, σ', spectra without and with muscovite mica. (b) Comparison of model predictions for the apparent imaginary dielectric permittivity, ε''_{app}, with experimental results.

indirectly influencing the bulk aspects of the copolymer. Figure 9a shows that in a homogeneous environment PVP-*co*-VAc presented a single broad relaxation process at the temperature presented, while for the heterogeneous system two relaxation processes are evident. Similar to the dynamics that occurred with glycerol (Figure 2a), it seems as if the single step in σ' for the homogeneous system gets transformed into two discrete steps for the heterogeneous system that encompass the same frequency range. Thus, the single relaxation process that occurs in the homogeneous system gets transformed to two relaxation processes in the presence of muscovite mica. Not shown is at higher temperatures two more polarization phenomena occur in the heterogeneous system, not including the conductivity wing, while the homogeneous system only displays a conductivity wing. Figure 9b demonstrates that none of the models were able to resolve either of the relaxation processes and only showed a limited region in which there was agreement with the experimental results. With the exception of the UWB and the Lichtenecker model for $\zeta = 1/2$ which predicted a single relaxation process, all the models were able to predict the presence of two relaxation processes, but their locations were underestimated.

Table 1 presents a summary of the quality of the predictions of the models investigated, and it is demonstrated that the models were limited in resolving the experimental dynamics. However, for most cases, ε''_{app} matched the experimental data in limited spectral windows. Though the physical arrangement of the condenser should, by assumption, coincide with the LWB, the authors were reluctant to press forward for a critical assessment of the deviation from the LWB without first assessing other models that encompass heterogeneous systems that fall within Weiner's bounds. These models represent systems where the electric field is neither parallel nor perpendicular to the condenser, and thus, effective geometries that represent such deviant behavior were considered. Of the molecules studied, it was noted that the polarization phenomena that occurred due to the presence of muscovite mica was of the slowest processes. An inference may be drawn from the results of DMSO (Figure 5a) and PMHS (Figure 7a) that the ionic characteristics of muscovite mica play a part in the resultant dynamics that were presented in this manuscript. This warrants a keen molecular analysis to appreciate the role substrates with negligible losses such as muscovite mica play in heterogeneous systems.

dx.doi.org/10.1021/jp211047j | J. Phys. Chem. B 2012, 116, 4346–4353

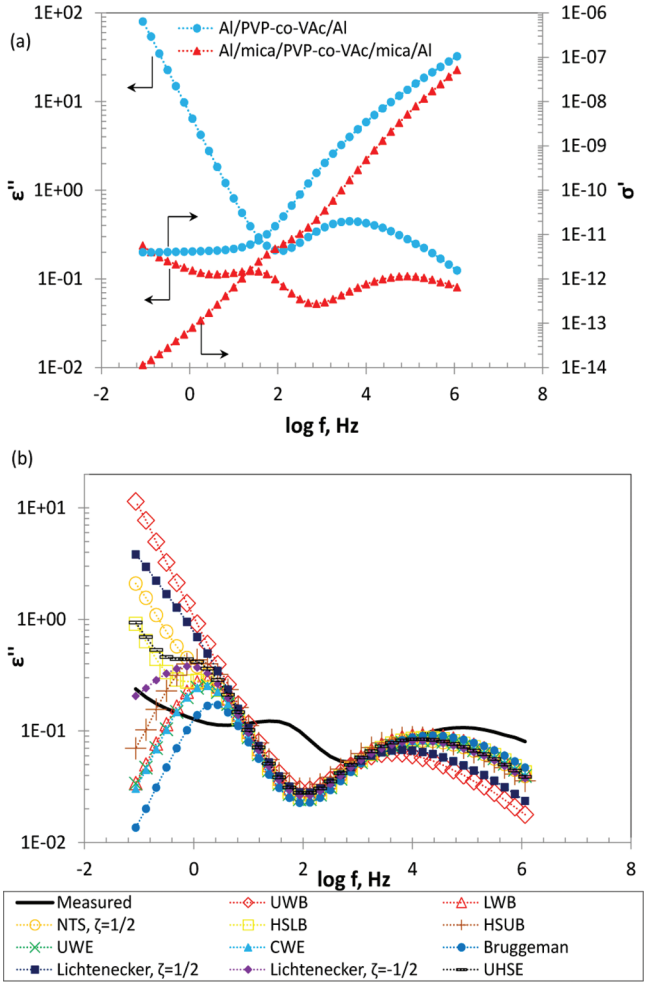

Figure 9. Dynamics of PVP-*co*-VAc at 160 °C. (a) Imaginary dielectric permittivity, ε'', and real conductivity, σ', spectra without and with muscovite mica. (b) Comparison of model predictions for the apparent imaginary dielectric permittivity, ε''_{app}, with experimental results.

CONCLUSION

Of the models investigated, the most successful were the HSUB, CWE, and Lichtenecker model for $\zeta = -1/2$. The least successful models were the UWB, NTS model for $\zeta = 1/2$ and Lichtenecker model for $\zeta = 1/2$. It should be recalled that the models that presented power law relationships were solved for the simple case of $\zeta = 1/2$ or $-1/2$ and that a plethora of other values could have been investigated, even though solving the models for the real and imaginary components of the apparent dielectric permittivity at values other than 1/2 or −1/2 would have been more challenging.

PLLA was the only molecule to have the resultant dynamics in a laminar heterogeneous configuration correctly predicted of the molecules investigated. The correct prediction was made by the Lichtenecker model for $\zeta = -1/2$. In all the other cases, none of the models were able to resolve the resultant dynamics but did present limited regions in which there was agreement with the experimental data.

Though the models were not able to resolve the dynamics of the molecules investigated—at the temperatures presented—in a laminar heterogeneous configuration oriented perpendicular to the applied electric field, the most successful of the models were able to locate the frequency at which the dielectric loss of a relaxation process was at a maximum. This is an important result. Even though the shape of the spectra could not be resolved, thermodynamic evaluation of the resulting relaxation processes is still possible. Of course, a molecular interpretation of the dynamics of a laminated heterogeneous system would still be warranted. This will be the focus of our next communication.

AUTHOR INFORMATION

Corresponding Author

*E-mail: rmcken01@students.poly.edu.

Notes

The authors declare no competing financial interest.

REFERENCES

(1) Arndt, M.; Stannarius, R.; Gorbatschow, W.; Kremer, F. *Phys. Rev. E* **1996**, *54*, 5377−5390.
(2) Gorbatschow, W.; Arndt, M.; Stannarius, R.; Kremer, F. *Europhys. Lett.* **1996**, *35*, 719−724.
(3) Schuller, J.; Richert, R.; Fischer, E. W. *Phys. Rev. B* **1995**, *52*, 15232−15238.
(4) Huwe, A.; Kremer, F.; Hartmann, L.; Kratzmuller, T.; Braun, H. G.; Karger, J.; Behrens, P.; Schwieger, W.; Ihlein, G.; Weib, O.; Schuth, F. *J. Phys. IV* **2000**, *10*, Pr7-59−Pr7-65.
(5) Serghei, A.; Kremer, F. *J. Chem. Phys.* **2009**, *131*, 154904-1−154904-10.
(6) Labahn, D.; Mix, R.; Schonhals, A. *Phys. Rev. E* **2009**, *79*, 011801-1−011801-9.

Table 1. Summary of Model Predictions in Comparison to Experimental Results for Each Molecule Studied[a]

	molecule							
model	glycerol	imidazole	phenyl salicylate	DMSO	PLLA	PMHS	PDLLA	PVP-*co*-VAc
UWB	-	-	-	-	-	-	-	-
LWB	-	-	-	-/K_2	-	-	-	-
NTS, $\zeta = 1/2$	-	-	-	-	-	-	-	-
HSLB	-/K_2	-	-	-/K_2	-	-	-	-
HSUB	-/K_2	-/K_1	-/K_1	-/K_2	-/K_1	-	-/K_1	-
UWE	-/K_2	-	-	-/K_2	-	-	-	-
CWE	-/K_2	-/K_1	-/K_1	-/K_2	-/K_1	-	-/K_1	-
Brugg.	-	-	-	-/K_2	-	-	-	-
Licht., $\zeta = 1/2$	-	-	-	-	-	-	-	-
Licht., $\zeta = -1/2$	-/K_2	-	-/K_1	-/K_2	+/K_1	-	-	-
UHSE, $\zeta = 1/2$	-/K_2	-	-	-/K_2	-	-	-	-

[a] +, full spectral resolution; -, limited spectral resolution; K_i, locates frequency of maximum dielectric loss for ith relaxation process.

(7) Cho, Y.-K.; Watanabe, H.; Granick, S. *J. Chem. Phys.* **1999**, *110*, 9688−9696.
(8) Serghei, A.; Kremer, F. *Rev. Sci. Instrum.* **2008**, *79*, 026101-1−026101-2.
(9) Serghei, A.; Tress, M.; Kremer, F. *Macromolecules* **2006**, *39*, 9385−9387.
(10) Capponi, S.; Napolitano, S.; Behrnd, N. R.; Couderc, G.; Hulliger, J.; Wubbenhorst, M. *J. Phys. Chem. C* **2010**, *114*, 16696−16699.
(11) Rotella, C.; Napolitano, S.; Wubbenhorst, M. *Macromolecules* **2009**, *42*, 1415−1417.
(12) Bergman, R.; Jansson, H.; Swenson, J. *J. Chem. Phys.* **2010**, *132*, 044504-1−044504-8.
(13) Jansson, H.; Bergman, R.; Swenson, J. *Phys. Rev. Lett.* **2010**, *104*, 017802-1−017802-4.
(14) Pizzitutti, F.; Bruni, F. *Rev. Sci. Instrum.* **2001**, *72*, 2502−2504.
(15) Pizzitutti, F.; Bruni, F. *Phys. Rev. E* **2001**, *64*, 052905-1−052905-4.
(16) Maxwell, J. C. *A Treatise on Electricity and Magnetism*; Dover Publications, Inc: Mineola, New York, 1954; Vol. *1*.
(17) Weiner, O. *Abh. Math.-Phys. Kon. Sach. Gesell. Wissen.* **1913**, *32*, 507−604.
(18) Garnett, J. C. M. *Philos. Trans. R. Soc.* **1904**, *203*, 385−420.
(19) Choy, T. C. *Effective Medium Theory: Principles and Applications*; Oxford University Press: New York, 1999.
(20) Bruggeman, D. A. G. *Ann. Phys.* **1935**, *24*, 636−679.
(21) Neelakantaswamy, P. S.; Turkman, R. I.; Sarkar, T. K. *Electron. Lett.* **1985**, *21*, 270−271.
(22) Lichtenecker, K. *Phys. Z.* **1924**, *25*, 169−181.
(23) Lichtenecker, K. *Kolloidchem. Beih.* **1926**, *23*, 285−291.
(24) Hashin, Z.; Shtrikman, S. *J. Appl. Phys.* **1962**, *33*, 3125−3131.
(25) Hashin, Z.; Shtrikman, S. *J. Mech. Phys. Solids* **1963**, *11*, 127−140.
(26) Richert, R. *Eur. Phys. J. E* **2009**, *68*, 197−200.
(27) Wagner, K. W. *Arch. Elektrotech.* **1914**, *2*, 371−387.
(28) Sillars, R. W. *Proc. IEEE- Wireless Section* **1937**, *12*, 139−155.
(29) Beek, L. K. H. v. Dielectric Behaviour of Heterogeneous Systems. In *Progress in Dielectrics*; The Chemical Rubber Company: Cleveland, Ohio, 1967; Vol. *7*, pp 69−114.
(30) Kremer, F.; Schönals, A. *Broadband Dielectric Spectroscopy*; Springer-Verlag: Berlin, Heidelberg, 2003.
(31) Wang, C. C; Lu, H. B.; Jin, K. J.; Yang, G. Z. *Mod. Phys. Lett. B* **2008**, *32*, 1297−1305.
(32) Richert, R. *J. Chem. Phys.* **2010**, *133*, 074502-1−074502-5.
(33) Dye, D. W.; Hartshorn, L. *Proc. Phys. Soc., London* **1924**, *37*, 42−57.
(34) Kudlik, A.; Benkhof, S.; Blochowicz, T.; Tschirwitz, C; Rössler, E. *J. Mol. Struct.* **1999**, *479*, 201−218.
(35) Dixon, P. K.; Wu, L.; Nagel, S. R. *Phys. Rev. Lett.* **1990**, *65*, 1108−1111.
(36) Barthel, J.; Bachhuber, K; Buchner, R.; Gill, J. B.; Kleebauer, M. *Chem. Phys. Lett.* **1990**, *167*, 62−66.
(37) Baessler, H.; Basel, G.; Berg, G.; Egle, S.; Riehl, N. *Phys. Status Solidi A* **1971**, *4*, 701−711.
(38) Bhattacharyya, K. G. *J. Electron Spectrosc.* **1993**, *63*, 289−306.
(39) Maslova, M. V.; Gerasimova, L. G.; Forsling, W. *Colloid J.* **2004**, *66*, 322−328.
(40) Mijovic, J.; Sy, J.-Y. *Macromolecules* **2002**, *35*, 6370−6376.
(41) Brás, A. R.; Viciosa, M. T.; Wang, Y.; Dionísio, M.; Mano, J. F. *Macromolecules* **2006**, *39*, 6513−6520.
(42) Arnoult, M.; Dargent, E.; Mano, J. F. *Polymer* **2007**, *48*, 1012−1019.